J Solid State Eletrochem (2003) 8: 66–72
DOI 10.1007/s10008-003-0398-4

ORIGINAL PAPER

R. Holze · Y. P. Wu

Novel composite anode materials for lithium ion batteries with low sensitivity towards humidity

Received: 15 November 2002 / Accepted: 11 June 2003 / Published online: 27 September 2003

Abstract Graphitic anode materials for lithium ion batteries processed under high humidity conditions show severe performance losses. The sensitivity of these materials towards humidity can be significantly reduced by adsorbing metal ions like silver or copper ions, with subsequent heat treatment of these composites. Results of X-ray photoelectron spectroscopy, high-resolution electron microscopy, thermogravimetry, and differential thermal analysis indicate that the deposited metals exist in metallic and carbide, M_xC (M = Cu or Ag), forms. They remove or cover (i.e. deactivate) active hydrophilic sites at the surface of the graphite. These composites absorb less water during processing. The electrochemical performance, including reversible capacity, coulombic efficiency in the first cycle, and cycling behavior, is markedly improved. This approach provides a potentially powerful method to manufacture lithium ion batteries under less demanding conditions.

Keywords Anode materials · Composite materials · Lithium ion batteries

Introduction

Because of their numerous advantages over traditional rechargeable systems like lead–acid and NiCd cells, lithium ion secondary batteries have established themselves successfully after technological breakthroughs concerning anode materials in the early 1990s. So far, a lot of anode materials has been studied; a considerable amount of this research has been devoted to the development of anode materials with a large reversible lithium capacity [1, 2]. Few studies have been focused on the environmental conditions for manufacturing lithium ion batteries, such as the composition of the atmosphere and in particular the water content, despite their importance on the performance of the batteries.

In this regard, the anode material is more important than the cathodic one, even though it is relatively cheaper, since its electrochemical performance, especially its cycling behavior, determines the cycling behavior of the cell almost completely. It is more sensitive towards humidity than cathode materials. At high humidity, anode materials will easily absorb water, resulting in fast fading of reversible capacity and causing poor cell performance. It is known that the water content in a manufacturing environment is very difficult to maintain at the desirably low level of essentially 0 ppm. If the sensitivity of the anode material towards humidity can be decreased, the requirements for controlling the water content in the manufacturing environment can be lowered, and thus lithium ion batteries can be manufactured cheaper under less demanding conditions.

The surface structure of graphite is usually different from the bulk structure and includes a lot of features such as edge planes, basal planes, surface functional groups, and defects [1, 2, 3]. Recent results pertaining to anode materials indicate that the surface structure is also of great importance for the electrochemical performance [3, 4, 5, 6, 7, 8, 9, 10, 11]. For example, slight oxidation of graphite by air, oxygen, carbon dioxide, ozone, solutions of $(NH_4)_2S_2O_8$, nitric acid, $Ce(SO_4)_2$ and H_2O_2, or fluorination by fluorine gas, will lead to the formation of an efficient passivating film, and prevent the movement of graphene molecules in the *a*-axis direction. In the case of common natural graphite, imperfections with high reactivity can be eliminated and

Presented at the 3rd International Meeting on Advanced Batteries and Accumulators, 16–20 June 2002, Brno, Czech Republic

R. Holze (✉) · Y. P. Wu
Institut für Chemie,
AG Elektrochemie,
Technische Universität Chemnitz,
09107 Chemnitz, Germany
E-mail: rudolf.holze@chemie.tu-chemnitz.de

Y. P. Wu
Division of Chemical Engineering,
INET, Tsinghua University,
102201 Beijing, China

more nanochannels or micropores are introduced [4, 5, 8, 9]. Consequently, the cycling performance and reversible capacity of the modified graphite improve considerably. Surface treatments of graphite such as dipping in polymer solutions of, for example, gelatin or epoxy resin, and treatment with iodine, also decrease the reactivity of the surface groups of graphite with electrolyte constituents during charge and discharge and result in a decrease of irreversible capacity [12, 13, 14]. It is also known that the surface of carbon can easily adsorb considerable amounts of, for example, oxygen, water, and carbon dioxide [3].

These results clearly indicate the importance of the surface structure and composition for the electrochemical performance of carbon anodes. Recently, we found that deposition of a metal on the surface of natural graphite markedly lowered the sensitivity of anode materials to humidity [15]. In the present paper we report a detailed study of the effect of copper and silver and their influence on the sensitivity towards humidity. When handled under high humidity conditions (about 1000 ppm), the electrochemical performance of the composites was very good. In contrast, the unmodified natural graphite exhibited poor performance, although its electrochemical behavior was good under low humidity conditions (< 100 ppm).

Experimental

Composite materials were prepared by the following procedure. Four 1 g pieces of common natural graphite (Beishu Graphite Plant, China, designated as LS17, $d_{002} = 33.51$ pm, $L_c = 1200$ pm, and average particle size 17 μm), mildly modified and standardized in our laboratory by soaking in an aqueous solution of KOH in order to remove mineral constituents, were dipped in 10 mL aqueous solutions of 0.6 mol/L and 1.6 mol/L $Cu(NO_3)_2$, and 0.3 mol/L and 0.8 mol/L $AgNO_3$, separately at room temperature overnight. This natural graphite showed good cycling behavior; we did not observe capacity fading in the first 10 cycles when the material was processed under low humidity (< 100 ppm). The mixtures were dried at 80 °C with stirring. In order to ensure copper and silver combined strongly with the graphite structure, the dried mixtures were heated in a tube furnace at 600 °C under flowing argon for 4 h. The prepared products were named A1, A2, B1, and B2, respectively.

X-ray photoelectron spectra (XPS) were obtained with an ES-300 spectrometer (Kratos, Japan). The relative contents of the various carbon species and of the metals at the surface of the natural graphite were calculated on the basis of the integrals of their X-ray photoelectron intensities. Thermogravimetry and differential thermal analysis (TG-DTA) were performed with a PCT-1 instrument (Beijing Analytical Instruments, China) under air; the heating rate was 20 °C/min. Prior to the measurement of high-resolution electron microscopy (HREM) with a JEM-200CX microscope (Jeol, Japan), the samples were uniformly dispersed on micronets with cavities of micrometer size. Electrochemical capacity was measured with a model cell that used lithium foil as the counter electrode, a solution of 1 mol/L $LiClO_4$ dissolved in a mixture of EC/DEC (v/v = 3:7) as the electrolyte, and a homemade porous polypropylene film as the separator. The working electrode was prepared by pressing a mixture of the graphitic material and 5 wt% poly(vinylidene fluoride) dissolved in *N*,*N*′-dimethylformamide (DMF) as the binder into pellets with a diameter of ca. 1 cm. The mass of these pellets averaged 10 mg and was precisely determined. After drying under vacuum at 120 °C overnight, the pellets were kept in an argon glove box with controlled humidity (about 1000 ppm) for 1 h; later they were assembled quickly into model cells under the same humidity condition. Electrochemical performance was measured galvanostatically with a CT2001A cell test instrument (Wuhan Land Electronic, China); discharge (intercalation process) and charge (deintercalation process) voltages were kept between 0.0 and 2.0 V versus Li^+/Li at 0.2 mA.

Results and discussion

X-ray photoelectron spectra of Cu_{2p} ($S = 3/2$) and Ag_{3d} ($S = 5/2$) in the composites A2 and B1 are shown in Fig. 1; selected results are summarized in Table 1. Copper does not exist as an oxide; instead it is present as metallic copper and copper carbide, corresponding to binding energy peaks at 934.7 eV (atomic ratio: 52.22%) and 933.4 eV (47.78%), respectively [16]. $Cu(NO_3)_2$ will decompose into copper oxides during heat treatment, and the copper oxides will be further reduced by carbon if the heat treatment temperature is high enough [17]. Silver also exists in two states: metallic silver and as a carbide, Ag_xC, corresponding to binding energy peaks at 368.6 and 367.5 eV. Their relative atomic contents are 63.46% and 36.54%, respectively. $AgNO_3$ decomposes easily and the silver produced from the decomposition partly reacted with the graphite to form silver carbide [17]. From the relative contents of the carbides of copper and silver it follows that copper binds stronger with the carbon structure than silver.

X-ray photoelectron spectra of C_{1s} in the natural graphite LS17 and the prepared composites A2 and B1 are shown in Fig. 2; selected results are again

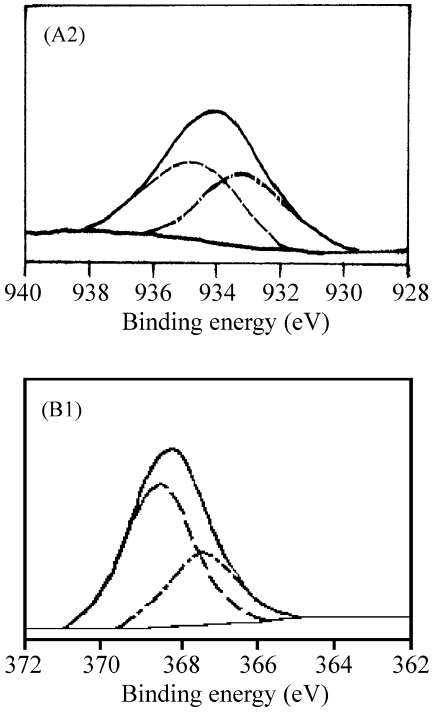

Fig. 1 XPS spectra of (**a**) Cu_{2p} ($S = 3/2$) and (**b**) Ag_{3d} ($S = 5/2$) in the composites A2 and B1

Table 1 Selected results for natural graphite LS17 and the prepared composites A1, A2, B1, and B2 from XPS measurements

Sample	Content of Cu or Ag (wt%)	Atomic ratio of silver species at different positions of the binding energy peaks (%)		Atomic ratio of carbon species at different positions of the binding energy peaks (%)		
		933.4 eV[a] 367.5 eV[b]	934.7 eV[a] 368.6 eV[b]	287.2 eV	286.0 eV	284.4 eV
LS17	0.0	–	–	6.10	9.02	80.50
A1	3.8	–	–	–	–	–
A2	10.2	47.78	52.22	5.02	12.34	79.75
B1	3.2	36.54	63.46	5.15	11.85	79.75
B2	8.6	–	–	–	–	–

[a]In the case of composites of Cu with LS17
[b]In the case of composites of Ag with LS17

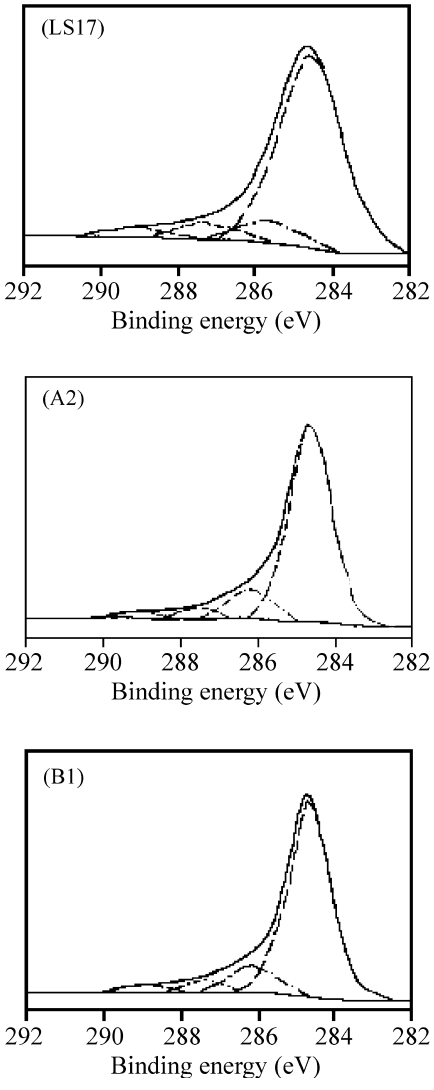

Fig. 2 XPS spectra of C_{1s} in natural graphite LS17 and in the composites A2 and B1

summarized in Table 1. Various carbon species exist at the surface of graphite, resulting in a complicated surface chemistry. Through deconvolution, four species are identified: carbonyl carbon, e.g. as in acetone/quinone, carboxylic carbon as in COOR (R = H and/or alkyl), ether carbon, and carbon atoms in graphene planes, corresponding to peaks of binding energy at 288.9, 287.2, 286.0, and 284.4 eV, respectively [18, 19]. The comparison between LS17 and the composites A2 and B1 shows that the content of carbon atoms with a binding energy peak of 286.0 eV increased from 9.02% to 12.34% (A2) and 11.85% (B1) but those of the others decreased. This increase indicates that copper and silver react with carbon to form carbides M_xC (M = Cu or Ag) with a peak position of the carbon atoms close to 286.0 eV, which is consistent with the above-mentioned XPS results for Cu_{2p} ($S = 3/2$) and Ag_{3d} ($S = 5/2$).

TG-DTA curves of natural graphite LS17 and the prepared composites A1, A2, B1, and B2 under air are shown in Fig. 3. Initially, the weight decreased slowly due to thermal decomposition of some oxides on the surface and slight oxidation, especially of reactive sites. Subsequently, when the temperature reached above 500 °C, significant oxidation began, indicated by substantial weight loss. The simultaneous rise of the DTA curves implies an exothermic reaction. When the rate of the combustion reaction peaked, the DTA curves passed through a maximum. Compared with natural graphite LS17, exothermal peaks observed with composites A1 and A2 under air shift sharply towards lower temperatures, from 752 °C to 686 °C and 637 °C, respectively. The composites B1 and B2 show the same behavior, with the exothermal peaks also shifting very sharply towards lower temperatures, 695 °C and 686 °C. It has been reported that metals or metal oxides such as Co, Ni, and Fe deposited on the surface of graphite can act as catalysts for oxidation and cause exothermal peaks to shift towards lower temperatures [5, 20, 21]. In these cases, Cu and Ag caused the same effect. A higher content of the deposited metal resulted in a lower value of the exothermal peak temperature. Of course, the shift between the various composites deposited with metals at different concentrations is not as pronounced as between natural graphite and the composites. The above results show clearly that the deposited copper and silver bonded strongly with the graphite structure, although our deposition method is different from previously reported ones [20, 21].

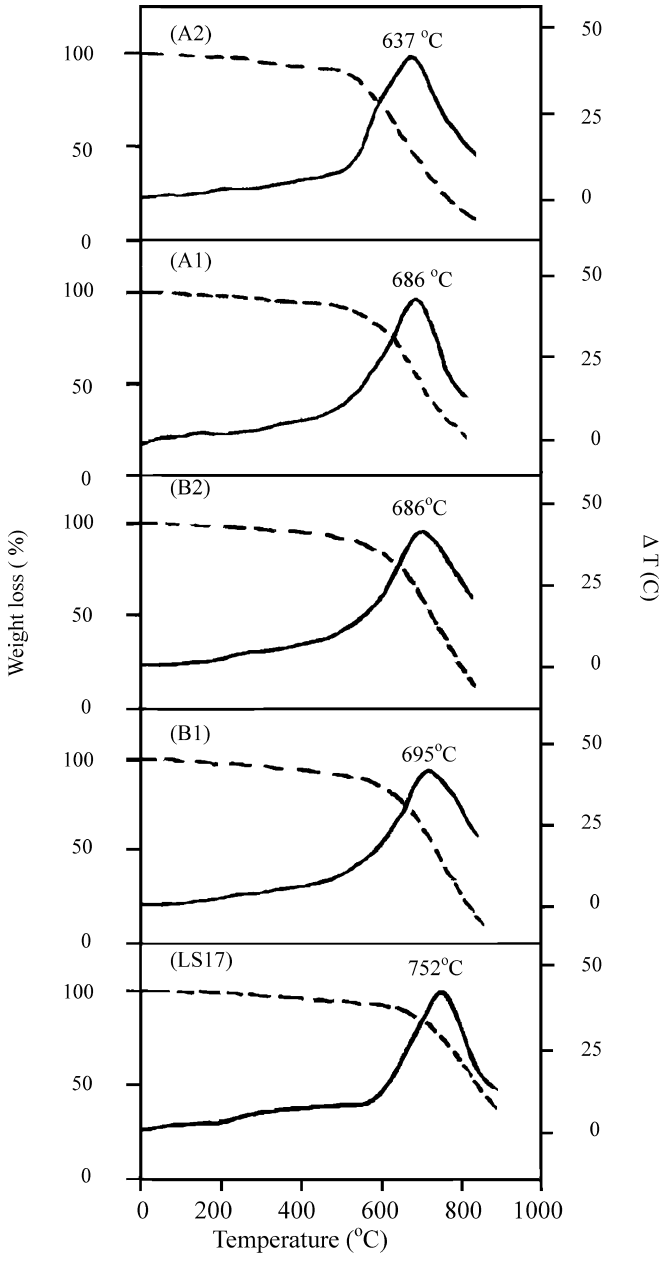

Fig. 3 TG-DTA curves for natural graphite LS17 and the composites A1, A2, B1, and B2 under air at $dT/dt = 20$ °C/min (*dashed lines*: TG curves; *full lines*: DTA curves)

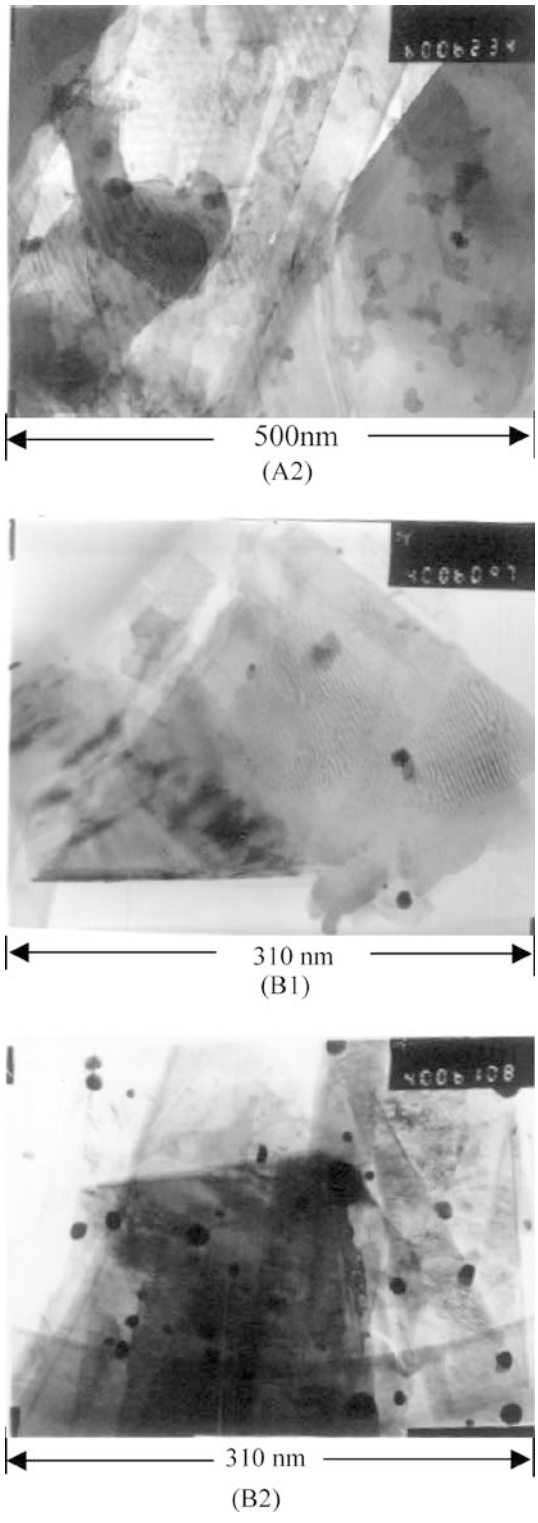

Fig. 4 HREM micrographs of composites A2, B1, and B2

In order to observe the distribution of the deposited metals on the surfaces of the composites, scanning electron microscopy was performed. No evidence of large metal clusters at the surface of natural graphite was obtained, presumably because the resolution was not high enough (the largest magnification was only 10,000:1). Of course, this does not prove that copper and silver were deposited homogeneously on the surface of graphite. High-resolution electron microscopy was additionally employed. The obtained micrographs are shown in Fig. 4. They indicate that the deposited copper and silver exist in nanometer-sized clusters or particles. Their size distribution is not very uniform. It is well known that there are some very active sites (also called hydrophilic sites) at the surface of natural graphite that adsorb water easily. They preferentially adsorb metal ions such as Cu^{2+} and Ag^{+} from the solutions. As a result, metal ions were concentrated at these hydrophilic sites. During the following heat treatment, the metal

ions reacted with carbon atoms at these active sites, producing metals and carbides M_xC (M = Cu or Ag), and thus metal clusters on the nanometer scale could be observed in the micrographs. The identification of their exact locations requires further studies, but we assume that they exist in both basal and edge planes since active hydrophilic sites are situated at both of them [3]. Of course, most of them are situated at the edge planes.

Discharge and charge profiles in the first cycle and discharge profiles in the second cycle of natural graphite LS17 and the composite materials (A1, A2, B1, and B2), manufactured into cells in the presence of high humidity (about 1000 ppm), are given in Fig. 5. The discharge capacity above 0.3 V in the first cycle for LS17 was a little higher than that for the composites A1, B1, and B2. Charge capacity (reversible capacity) changed from 320 to 324, 348, 321, and 333 mAh/g for A1, A2, B1, and B2, respectively. The coulombic efficiency in the first cycle was different: it increased subsequently from 77.8% to > 83%. When natural graphite LS17 was built into cells under low humidity conditions (< 100 ppm), its reversible capacity was 335 mAh/g and the coulombic efficiency in the first cycle was 88.5%. The time interval that the anode materials were exposed to the high humidity environment was not very long (1 h); the absorbed amount of water prior to the assembling was accordingly limited. However, this amount of water had a great influence on lithium intercalation. Lithium usually intercalates via the edge planes. With anode pellets prepared under low humidity conditions, lithium intercalation was favored by defects including hydrophilic sites at edges because more passages remain available. However, when the active hydrophilic sites were occupied by water, this water was electrochemically reduced or reacted with lithium ions in the electrolyte or some components of the surface film from electrochemical reduction of the electrolyte solvents such as EC and DEC to produce LiOH or other types of compounds such as ROH [22, 23], and the following lithium intercalation was not favored at these defect sites. In addition, part of the absorbed water could diffuse into the electrolyte solution before lithium intercalation since the anode pellets were in contact with the electrolyte solution for some time before the capacity measurement. This diffusion increased the ionic conductivity of the organic solution, and thus enhanced electrochemical reduction of the electrolyte at the interface between graphite and the organic solution as a side reaction [22]. This enhanced side reaction made the passivating film thicker and did not favor lithium intercalation, since a longer diffusion distance was required for lithium to intercalate [22]. Moreover, after formation of the passivating film, part of the water might have came back to react with constituents of the formed film such as lithium alkyl carbonate, producing LiOH and ROH [1, 22, 23]. This reaction caused the usual compact film to become loose or more porous, and thus solvated lithium ions could also co-intercalate [22]. As a result, the reversible capacity of LS17 under high humidity conditions was lowered, from 335 to 320 mAh/g, and the coulombic efficiency in the first cycle decreased from 88.5% to 77.8%.

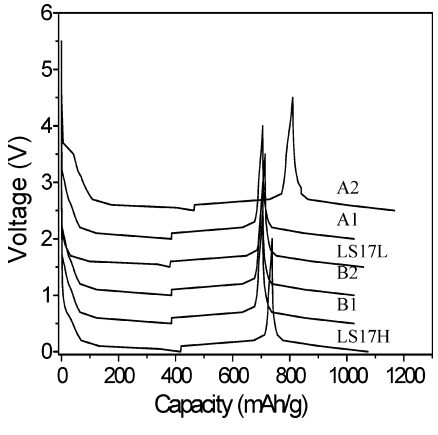

Fig. 5 Discharge and charge curves in the first cycle and discharge curves in the second cycle for natural graphite LS17 and composites A1, A2, B1, and B2. For clarity, the voltages for B1, B2, LS17L, A1, and A2 are shifted upwards by 0.5, 1.0, 1.5, 2.0, and 2.5 V, respectively

The above results clearly show that in the presence of high humidity the reversible lithium capacity was enhanced after copper or silver were deposited onto the surface of natural graphite. From the discharge profiles in the first cycle of composites A1 and A2, it can be seen that there is a slope between 0.8 and 0.3 V. This slope enhances with the amount of copper deposited, and in the case of A2 it is longer than that for LS17 under high humidity. Evidently one reasonable possibility is that it is from the alloying between Li and Cu, though from the charge profiles we could not observe any clear evidence of the decomposition of the alloys. In addition, the charge capacity also increases with the deposited amount of copper, and is higher than that of LS17 at low humidity when the deposited amount of copper is 10.2%. From this result, the contribution of the deposited copper to the reversible capacity could not be denied. Recent studies showed that there is also reversible discharging and charging between 1.0 and 0.02 V vs. Li^+/Li for CuO particles, which is beyond the well-known region (> 1 V) for lithium intercalation into CuO and Cu_2O [24]. Unfortunately, this phenomenon was not fully investigated, but it clearly shows there are other factors associated with copper. In our case, the size of copper clusters is in the nanometer range. The physicochemical properties of nanometer materials are quite different from those of larger particles. For example, metal tin plate cannot act as a good matrix for lithium storage. However, when its particle size becomes smaller, its reversible capacity enhances greatly, especially when its size is in the nanometer range, and becomes very high [25]. Our results suggest that the nanosize-deposited copper clusters are effective as a matrix for lithium storage [26, 27], although a copper foil/thin film could not act as a matrix for lithium storage [28].

In the case of silver, from the discharge and charge profiles we could not see any clear evidence of alloying between Li and Ag. Furthermore, its reversible capacity was not above that of the pure natural graphite (LS17) handled at low humidity, even when the content of the deposited silver was up to 8.6%. Consequently, the contribution of the deposited silver to the reversible capacity cannot be determined precisely. However, since silver can reversibly form alloys with lithium below 0.3 V, the same voltage range as that for lithium to intercalate into graphite [29, 30], we assume that silver also contributed to the reversible capacity like copper since it also increases with the silver content. Certainly, further studies aimed in particular at identification of Li_xAg after discharge are necessary.

Deposited metals such as Ni and Al can block the access of electrolytes to the edge planes [31, 32], and the deposited copper and silver would have acted in the same way to impede the decomposition of the electrolytes; therefore coulombic efficiency in the first cycle increased.

Cycling behavior in the first 10 cycles of natural graphite LS17 and the composite anode materials (A1, A2, B1, and B2) are shown in Fig. 6.. In the case of LS17, when the cells were built under low humidity (curve LS17L), its reversible capacity did not fade in the first 10 cycles. In the presence of high humidity, its reversible capacity faded very quickly in the first 10 cycles, from 320 to 230 mAh/g (curve LS17H). In the case of composites A1 and A2, there is no evident fading in capacity with cycle number when handled under high humidity conditions. With composite materials B1 and B2, the cycling behavior was different. With B1 the capacity did not fade very quickly at first, but later faded to almost the same level as that of LS17. With B2 there was no evident capacity fading in the first 10 cycles in the presence of high humidity, which is similar to the behavior of LS17 under low humidity.

As mentioned above, the reaction between water and lithium alkyl carbonate, the main component of the passivating film on lithium surfaces, produced LiOH and ROH [1, 5, 22, 23, 33], and this kind of reaction made the passivating film at the surface of natural graphite loose and porous, with possible co-intercalation of solvated lithium ions, though EC is regarded as a good solvent for graphitic carbon [1]. This resulted in exfoliation of graphene planes and a consequent fading in capacity [34]. After the deposition of copper and silver, active hydrophilic sites at the surface of natural graphite were blocked, the amount of adsorbed water decreased sharply, and the cycling behavior improved strikingly. As deduced from the above-mentioned results of the TG-DTA measurements, the strong binding between the deposited copper and silver and the graphite structure perhaps also contributed to this good cycling behavior, which deserves further study.

Owing to the higher positive charge density of Cu^{2+}, the interaction of copper ions with active hydrophilic sites at the surface of graphite is stronger than that of silver ions, and thus more active sites can be covered/removed. Consequently, the electrochemical performance of the composites of the former with graphite is a little superior to that of the latter.

With respect to the effect of the deposited metals on an increase in electronic conductivity, perhaps they will favor lithium intercalation or diffusion like coated Ni, and thus the high rate capability will also improve [31]. As to other conceivable roles of metals and carbides, further studies are necessary.

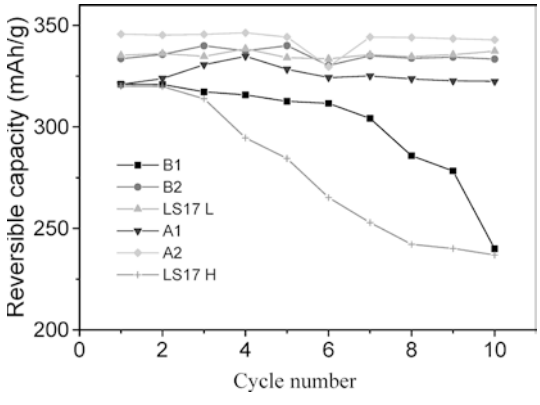

Fig. 6 Cycling behavior of natural graphite LS17 and the prepared composites A1, A2, B1, and B2. The curve labeled *LS17L* was obtained with LS17 processed under low humidity (below 100 ppm) conditions; the other curves were obtained with materials processed under high humidity (about 1000 ppm) conditions

Conclusions

In summary, there are active hydrophilic sites at the surface of natural graphite. They preferentially adsorb metal ions from solutions. After heat treatment they can be covered/removed effectively by the absorbed metal ions through formation of metals and metal carbides, M_xC (M = Cu or Ag). The deposited metals exist in nanometer clusters. Consequently, when cells are assembled in the presence of high humidity (about 1000 ppm), the composite materials of natural graphite with the deposited metals adsorb markedly less water and provide good electrochemical performance. This method is promising for industry to manufacture lithium ion batteries under less critical conditions.

Acknowledgements Financial support from the China Postdoctor Foundation and the Alexander von Humboldt Foundation is appreciated.

References

1. Besenhard JO (1999) Handbook of battery materials. Wiley-VCH, Weinheim
2. Wu YP, Wan C, Jiang C, Fang SB (2002) Principles, introduction and advances of lithium secondary batteries. Tsinghua University Press, Beijing

3. McCreery RL (1991) Carbon electrodes: structural effects on electron transfer kinetics. In: Bard AJ (ed) Electroanalytical chemistry, vol.17. Dekker, New York, p 221
4. Peled E, Menachem C, Bar-Tow D, Melman A (1996) J Electrochem Soc 143:L4
5. Wu YP, Wan C, Jiang C, Tsuchida E (2000) Electrochem Commun 2:272
6. Takamura T, Awano H, Ura T, Sumiya K (1997) J Power Sources 68:114
7. Ein-Eli Y, Koch VR (1997) J Electrochem Soc 144:2968
8. Wu YP, Jiang C, Wan C, Tsuchida E (2001) J Mater Chem 11:1233
9. Wu YP, Jiang C, Wan C, Holze R (2003) J Appl Electrochem (in press)
10. Menachem C, Wang Y, Floners J, Peled E, Greenbaum SG (1998) J Power Sources 76:180
11. Nakajima T, Yanagida K (1996) Tanso 174:195
12. Gaberscek M, Bele M, Drofenik J, Dominko R, Pejovnik S (2000) Electrochem Solid-State Lett 3:171
13. Saito M, Sumiya K, Sekine K, Takamura T (1999) Electrochemistry 67:957
14. Wang H, Yoshio M (2001) J Power Sources 101:35
15. Wu YP, Jiang C, Wan C, Tsuchida E (2000) Electrochem Commun 2:626
16. Barbooti M (1984) Sol Energy Mater 10:35
17. Vinkevisius J, Mozginsiene I, Jasulatiene V (1998) J Electroanal Chem 442:73
18. Wu Z, Pittman CU, Gardner SD (1995) Carbon 33:597
19. Zielke U, Huttinger KJ, Hoffman WP (1996) Carbon 34:983
20. Goethel PJ, Yang RT (1989) J Catal 119:201
21. Oh SG, Baker R (1991) J Catal 128:137
22. Pyun SI (1999) Fresenius J Anal Chem 363:38
23. Aurbach D, Ein-Eli Y, Chusid O, Carmeli Y, Babai M, Yamin H (1994) J Electrochem Soc 141:603
24. Debart A, Dupont L, Poizot P, Leriche JB, Tarascon J (2001) J Electrochem Soc 148:A1266
25. Whitehead A, Ellioft J, Owen J (1999) J Power Sources 81–82:33
26. Huang H, Kelder EM, Schoonman J (2001) J Power Sources 97–98:114
27. Grugeon S, Laruelle S, Herrera-Urbina R, Dupont L, Poizot P, Tarascon JM (2001) J Electrochem Soc 148:A285
28. Suzuki J, Yoshida M, Nakahara C, Sekine K, Kikuchi M, Takamura T (2001) Electrochem Solid-State Lett 4:A1
29. Momose H, Honbo H, Takeuchi S, Nishimura K, Horiba T, Muranaka Y, et al. (1997) J Power Sources 68:208
30. Nishimura K, Honbo H, Takeuchi S, Horiba T, Oda M, Koseki M, et al. (1997) J Power Sources 68:436
31. Yu P, Ritter JA, White RE, Popov BN (2000) J Electrochem Soc 147:1280
32. Kim S, Kadoma Y, Ikuta H, Uchimoto Y, Wakihara M (2001) Electrochem Solid-State Lett 4:A109
33. Dolle M, Grugeon S, Beaudoin B, Dupont L, Tarascon JM (2001) J Power Sources 97–98:104
34. Chung GC, Jun SH, Lee KY, Kim MH (1999) J Electrochem Soc 146:1664